IOP Conference Series: Materials Science and Engineering

A flow forming process model to predict workpiece properties in AISI 304L

IOP Conf. Series: Materials Science and Engineering 1270 (2022) 012093 doi:10.1088/1757-899X/1270/1/012093

A flow forming process model to predict workpiece properties in AISI 304L

B Arian[1,*], A Oesterwinter[1], W Homberg[1], J R Vasquez[2], F Walther[2], L Kersting[3] and A Trächtler[3]
[1] Forming and Machining Technology (LUF), Paderborn University, Paderborn, Germany
[2] Chair of Materials Test Engineering (WPT), TU Dortmund University, Dortmund, Germany
[3] Fraunhofer Institute for Mechatronic Systems Design (IEM), Paderborn, Germany
[*] Corresponding author: E-mail: ba@luf.uni-paderborn.de

Abstract. The control of workpiece properties enables an application-oriented and time-efficient production of components. In reverse flow forming, e.g., the control of the microstructure profile, in contrast to the adjustment of the geometry, is not yet part of the state of the art. This is particularly challenging when forming seamless tubes made of metastable austenitic stainless AISI 304L steel. In this steel, a phase transformation from austenite to martensite can occur due to mechanically and/or thermally induced energy. The α'-martensite has different mechanical and micromagnetic properties, which can be advantageous depending on the application. For the purpose of local property control, the resulting α'-martensite content should be measured and controlled online during the forming process. In this paper, results from an empirical correlation model of process parameter combinations and resulting α'-martensite content as well as geometry will be presented. Based on this, the focus of the paper will be on process modeling by means of FEM in order to create the transition to a numerically supported process model. Furthermore, it will be specified how the numerical process model can be used in a predictive manner for an online closed-loop process control.

1. Introduction

The requirements on materials, tools and processes in manufacturing companies are increasing as a result of growing customer demands [1]. For this reason, the reproducible production of (complex) defect-free components is one of the main objectives of production and manufacturing technology geared to meeting customer needs while, at the same time, conserving resources [2]. In this context, the production of components tailored to customer requirements is taking on increasing importance. This requires a stable process in which the input variables (e.g. process parameters and semi-finished product) can be defined and the output variables (e.g. geometry and workpiece properties) can ideally be predetermined. The process of reverse flow forming is hard to predict in respect of the stress and strain distribution, for example, and is affected by a large number of influencing factors [3]. While geometry control (e.g. wall thickness) is already possible in reverse flow forming, the adjustment of local workpiece properties (e.g. microstructure profile) still constitutes a challenge. This is particularly complicated for seamless tubes made of metastable austenitic stainless steel, such as AISI 304L (X2CrNi18-9, 1.4307) as semi-finished products. The metastable austenitic phase is not in an equilibrium state and can thus be transformed through deformation- or temperature-induced energy into α'-martensite with different mechanical and magnetic properties [4, 5]. A promising approach in this context is closed-loop process control. Initial experimental investigations conducted for subsequent application in the closed-loop process control of α'-martensite content for metastable austenitic stainless AISI 304L steel during flow forming were carried out as part of a priority program funded by the DFG.

The investigations were performed jointly by Forming and Machining Technology (LUF, Paderborn University), the Chair of Materials Test Engineering (WPT, TU Dortmund University) and the Fraunhofer Institute for Mechatronic Systems Design (IEM, Paderborn). These served to identify correlations between flow forming process parameters and the resulting strain-induced α'-martensite content as well as the true strain φ_r (true strain in thickness direction) of the formed seamless tubes [6]. In this way, it was possible to develop empirically-determined correlation models (see section 2.3), one of which is shown in Figure 1 as an example, which are to be incorporated as a database into the envisaged closed-loop process control.

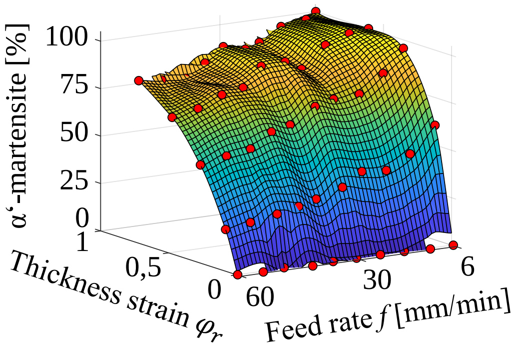

Figure 1. Results of α'-martensite content (vol.-%) over thickness strain φ_r as a function of reduction per pass and feed rate f.

In order to achieve the transition from this purely data-driven model to a numerically supported model, the FEM is to be used in a predictive manner. This way, a process model is to be developed which makes it possible to predict the occurring strain distribution as well as the α'-martensite content in locally restricted workpiece areas. In the proposed paper, the focus will be on process modeling by means of the FEM for reverse flow forming. The resulting boundary conditions of the process are to be considered in the model. The essential parameters of the process, such as the feed rate f and the infeed Δr, must be adjustable in order to allow simulation of different process settings. In addition, the work hardening and resulting α'-martensite formation are to be considered and integrated into the calculation during the simulation of the flow stress. This change in the material property is to be incorporated using a specific subroutine.

2. Principles and experimental setup

2.1. Flow forming and application

As an incremental forming process flow forming is offering various advantages in terms of flexibility and efficiency [7]. By the intended wall thickness reduction tubular parts with excellent shape, dimensional accuracy and outstanding surface qualities can be produced [8]. Therefore, flow formed tubes meet the highest requirements, such as the standards of the aerospace industry. The components are used industrially in drive shafts for jet engines or helicopters, just to name a few [9]. In the scope of this paper, the focus is on reverse flow forming, where the material flows in the opposite direction to the roller tools movement [10].

2.2. Experimental preliminary work and objective

The series of experiments carried out previously took place on the flow forming machine BD 40 from Bohner-Köhle illustrated in Figure 2. Within the used machine configuration three co-rotating roller tools generated the necessary deformation forces for the wall thickness reduction. The roller tools were arranged at an angle of 120° to each other and moved axially along the workpiece while offering the possibility of an infeed Δr (radial movement). In terms of the dimensions the used roller tools have an outer diameter of 155 mm, an attack angle of α = 12°, an exit angle of β = 5° and a transition radius of R = 2 mm. The tube, which was to be plastically deformed, was placed on a spinning mandrel with an outer diameter of 72 mm. Typically, several passes are included for the forming process [11]. Metastable austenitic stainless steel AISI 304L was to be used as material for the seamless tubes with an initial outer diameter of 80 mm, a wall thickness w_0 of 4 mm and a length l_0 between 210 and 230 mm. The experiments, on which the correlation model is based, were performed isothermally at room temperature level T, which is in fact often the case with this process like Bylya et al. [11] already mentioned, at a constant rotational speed n of 30 rpm. Infeeds Δr of 0.5, 0.75 and 1 mm/pass with feed rates f between 6 and 60 mm/min in steps of 6 mm/min were used.

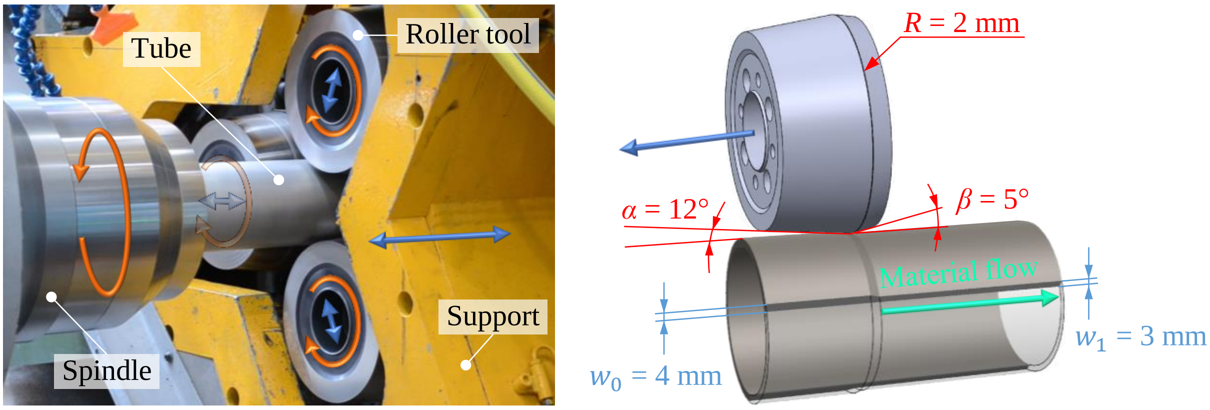

Figure 2. Flow forming machine setup (BD 40 from Bohner-Köhle).

The experiments from preliminary work pursued an empirical approach to process modeling. Correlation models (see section 2.3) were developed to quantify the influence of isolated process parameter variations, such as the feed rate or the wall thickness reduction per pass (infeed of the roller tools), on the resulting true strain φ_r (true strain in thickness direction) as well as the α'-martensite content, like mentioned in the introduction [6]. In addition to the process analysis, the correlations are used for model-based control design purposes. As part of the work presented here, it is to be investigated whether the occurring strain-induced phase transformation inside the material can be included within a FE process model. For this purpose, a specific process parameter setting (see section 2.4) from the previously performed experiments, mentioned above, is selected, which is used as an example to demonstrate the FEM-sided implementation.

2.3. Phase transformation of metastable austenite into α'-martensite

The stainless steel AISI 304L is a high-alloy austenitic steel composed of the metastable austenite phase (γ). As mentioned before, the phase transformation from metastable austenite into α'-martensite occurs in two different ways: Strain-induced triggered by means of mechanical deformation or temperature-induced as it is common in heat treatments [12].

The formation of α'-martensite during plastic deformation have been modelled using sigmoidal equations with horizontal asymptotes to describe the phase saturation. A classical model was proposed by Olson and Cohen in 1975 which describes the nucleation and growth of strain-induced α'-martensite related to the formation of deformation bands. The intersection points of these deformation bands are the nucleation points of α'-martensite [13]. Further models have included effects of the stress state [14] and the cumulative plastic strain during fatigue testing [15]. Inspired on those investigations, the authors proposed a first material model approach to describe the phase transformation during reverse flow forming of tubes. The model is represented by the equation (1) and it was developed based on empirical data. This equation allows the computation of the α'-martensite content considering the effects of the true strain φ_r in thickness direction and the feed rate f used during the production process [9].

$$\alpha' = \left[A_0 + A_1 \exp\left(\frac{\varphi}{A_2}\right)\right][B_0 + B_1\, f] \tag{1}$$

IOP Conf. Series: Materials Science and Engineering 1270 (2022) 012093 doi:10.1088/1757-899X/1270/1/012093

To compute the coefficients A_0, A_1, A_2, B_0 and B_1, data fitting routines in MATLAB were developed. Using the experimental data and considering the equation (1) as the ansatz function, the numerical values of the coefficients were calculated. As an example, for specimens produced with an infeed of 1 mm/pass, Figure 3(a) shows the experimental data. Introducing the calculated coefficients in equation (1), it is possible to plot the modelled 3D surface shown in Figure 3(b).

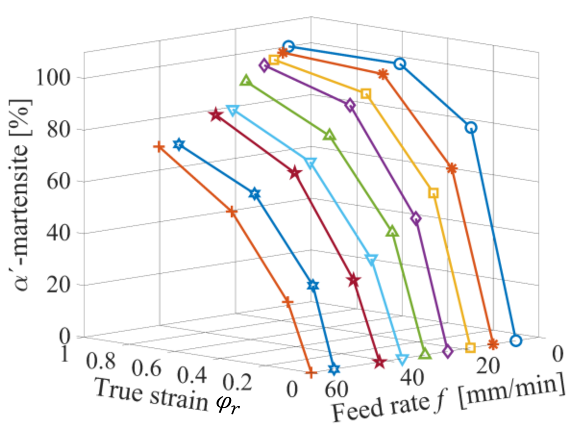

Figure 3. Results of α'-martensite content (vol.-%) as a function of the true strain φ_r and the feed rate f in specimens produced using an infeed of 1 mm/pass: (a) experimental data; (b) 3D surface model.

As mentioned in section 2.2, three different infeeds (0.5, 0.75 and 1 mm/pass) were used to produce the specimens. This means that three different groups of experimental data were fitted independently to obtain the respective equation and therefore the 3D surface models. Table 1 shows the numerical values of the coefficients computed for each group of data.

Table 1. Coefficients of the model equation (1) for different infeeds.

	Coefficients of model equation				
Infeed [mm/pass]	A_0	A_1	A_2	B_0	B_1
0.5	100.34	-100.28	0.19	1.12	-0,004
0.75	99.98	-99.78	0.21	1.09	-0.005
1.0	107.4	-107.67	0.2	1.05	-0.006

Using these coefficients on equation (1), a series of 3D surfaces can be plotted, as shown in Figure 4. These surfaces show the α'-martensite content during flow forming of metastable austenitic steel tubes, with respect to the true strain φ_r and the feed rate f for three different infeeds of the roller tool. Future work will focus on the inclusion of the infeed value as a variable, to develop an expanded model to increase the scope of validity.

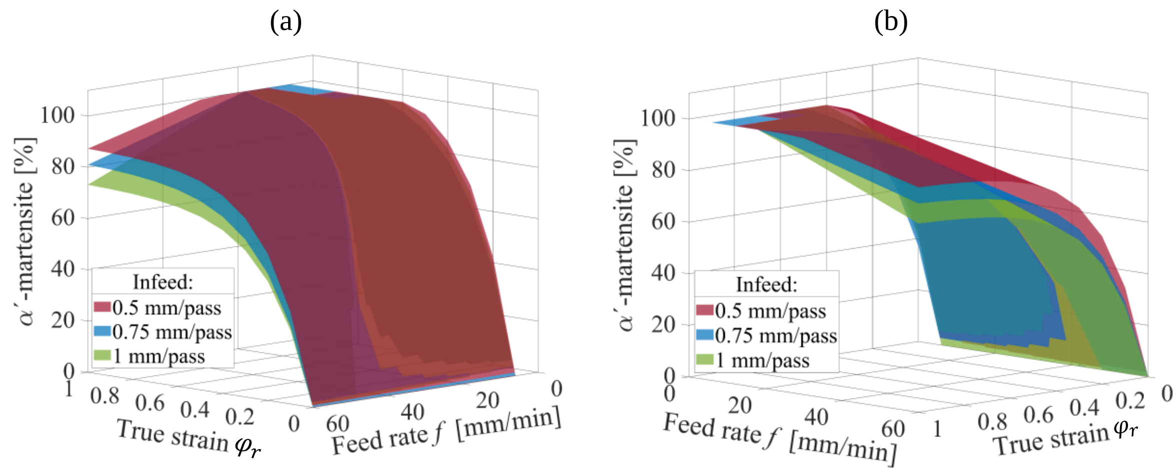

Figure 4. Plots of 3D surface models of α’-martensite content (vol.-%) as a function of the true strain φ_r and the feed rate f including three different infeeds: Perspective (a) (-135°, 10°); (b) (135°, 10°).

2.4. Application of FE modeling for flow forming

The main focus of the investigations in this paper is the establishment of an FE model of reverse flow forming, which takes into consideration the analytical α’-martensite formation as well as the associated hardening and enables both a radial and axial analysis thereof. For this purpose, the determination of simulative boundary conditions and requirements for the comprehensive representation of the reverse flow forming process and the associated object of investigation is necessary.

The process complexity requires an initial restriction within the scope of FE modeling. The model described in section 3 is valid for a wall thickness reduction respectively infeed of 1 mm, which is realized by a single pass. In addition, a constant rotational speed of 30 rpm, a constant feed rate of 60 mm/min and isothermal conditions at room temperature level are also assumed.

The FE process model is set up as a purely mechanical simulation of a dynamic problem. Thermal effects associated with the forming process are neglected. The thermo-mechanical coupling of the model represents an interesting object of investigation. However, since the thermal effects are small for the process variant considered here, among other things due to the use of cooling lubricant and isothermal conditions, neglecting them is justified. Due to the high nonlinearities of the process, an explicit time integration is necessary. The nonlinearities result i.a. from the large plastic deformations which the component undergoes and the constantly changing contact situation between the roller tools and the rotating tool.

In addition to the time integration, the space discretization of the reverse flow forming also represents an important boundary condition of the modeling. The classical Lagrangian mesh approach is no longer sufficient due to the high degrees of deformation, since a sufficiently fine element edge size has an extremely negative influence on the maximum permissible time step. The high degrees of deformation are thus associated with a large element deformation and thus with a negative influence on the solution quality. In addition to the pure Lagrangian mesh approach, there are a variety of other approaches for space discretization, such as adaptive remeshing or the use of discretization by means of Eulerian approach and the combination of both approaches by means of Arbitrary Lagrangian Eulerian (ALE) or Coupled-Euler-Lagrange (CEL). For the FE model described in section 3, the CEL discretization was used. The investigation of alternative space discretization options, the need for which is discussed in section 4, is a future research focus.

One goal of the FE modeling is to account for the α’-martensite formation that occurs during forming. Commercial FE programs such as ABAQUS/CAE and LS-DYNA certainly have material modeling that includes phase transformation. However, the analytical α’-martensite formation of the reverse flow forming process described in section 2.3 and the resulting work hardening shall be included here. This is implemented in the form of a subroutine, which is described in more detail in section 3.

3. FE modeling of the reverse flow forming process

To realize the requirements described in section 2.3, a FE process model is developed, which is described in more detail below.

The modeling is performed with the FE software ABAQUS/EXPLICIT. This offers a user interface in the form of subroutines, which allows the user to intervene at numerous points of the FE analysis, e.g., to generate custom material models or outputs. The subroutine type VUHARD is used for the representation of the α'-martensite formation as well as the work hardening. In addition, solution-dependent state variables, which can be defined within the subroutine, allow, among other things, the element-by-element reading and plotting of user variables, such as the α'-martensite content [16].

As described in section 2.4, the CEL approach is used to mesh the model. The intent of this approach is to avoid mesh problems when performing simulations that involve high deformations. This approach requires the definition of an additional Eulerian part. The FE modeling includes all relevant active surfaces of the reverse flow forming, which are listed in Figure 5: The tube, the Eulerian part, the mandrel and the roller tools.

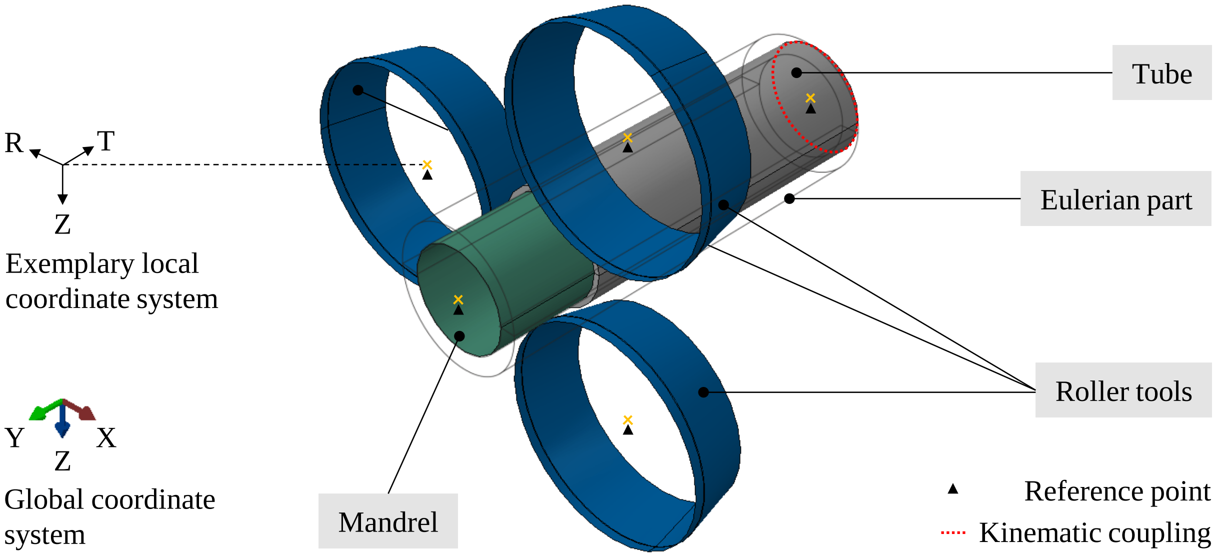

Figure 5. Reverse flow forming FE process model.

The semi-finished product is defined as a 3D deformable solid. Its Lagrangian mesh is meshed with C3D8R elements. The aspect ratio of these elements is slightly distorted in order to be able to map four elements over the wall thickness. Thus, the elements have a height of 1 mm and a width of 2 mm. A possibly resulting impairment of the solution quality is tolerated, since a finer discretization would increase the computation time significantly. The calculation times of the modeling and the influence of the subroutine on them will be discussed in more detail in section 4.

The semi-finished product is also subject to displacement boundary conditions, which are applied as a kinematic coupling to the reference point, which is shown in Figure 5. The translational degree of freedom (dof) in the y-direction is completely blocked, corresponding to the mechanical stop in the real process. In addition, the semi-finished product is rotated around the y-axis respectively its center axis. The semi-finished product is assigned an elastoplastic material whose characteristic values with density $\rho = 7.9 \cdot 10^{-3} \frac{g}{mm^3}$, Young's modulus $E = 2 \cdot 10^5\ MPa$ and Poisson's ratio $\upsilon = 0.2$ correspond to the material austenitic stainless steel AISI 304L. A yield curve is not given here since it is determined by the subroutine. The deformation of the semi-finished product must lie completely in the Eulerian part over the entire calculation time. Therefore, both the length and the outer diameter of this part are larger than those of the semi-finished product and the Eulerian part is penetrated by the roller tools in Figure **5**. This is meshed with EC3D8R elements.

The tools, consisting of the mandrel and three roller tools, are defined as 3D analytical rigid surfaces. This has the advantage that these parts do not have to be meshed, which has a positive effect on the calculation time. However, the assumption of a completely rigid material behavior represents an idealization, since stiffnesses of the system as well as elastic and plastic behavior of the tools are neglected. Therefore, it can be assumed that the FE modeling tends to overestimate stresses and strains. Moreover, the definition of the tools as 3D analytical rigid surfaces requires the definition of a reference point to give up boundary conditions. In the case of the displacement boundary conditions of the mandrel, all translational and rotational degrees of freedom are fixed. In addition to the reference points, a separate local coordinate system is also defined for each of the rollers, which can also be seen in Figure 5. When assigning displacement boundary conditions, a distinction must be made between the roller tools infeed step and the forming step. During the first step, the translational degree of freedom in the z-direction and the rotational degrees of freedom in the r- and z-directions are locked. In the second step, the translational degree of freedom in the r-direction is additionally locked and the feed in the t-direction is applied. Due to the frictional contact definition of the roller tools with the semi-finished product, the mass, the inertias and the moments of inertia at the reference points must be given up for the roller tools. In the FE model, a distinction is made between two contact situations, the contact between the semi-finished product and the mandrel and the before mentioned contact between the roller tools and the semi-finished product. The former is idealized and assumed to be frictionless. Friction is considered for the contact between the roller tools and the semi-finished product since these are not driven externally and are set in rotation solely due to the acting sliding friction. Coulomb's law of friction with a coefficient of friction of $\mu = 0.01$ is assumed for the lubricated contact of steel on steel.
The calculation within the subroutine can be divided into the α'-martensite formation and the hardening calculation. For this study, the α'-martensite formation according to section 2.3 was implemented for a wall thickness reduction Δw of 1 mm, the associated parameters are listed in Table 2. The α'-martensite content is calculated via equation (2) based on equation (1) (see section 2.3).

$$V_m = 107{,}4\ \left[1 - \exp\left(\frac{\varphi}{0.2}\right)\right][1.05 - 0.006f] \tag{2}$$

The combination of the parameters A_0 and A_1 prevents equation (2) from assuming a negative result for $\varphi = 0$.
It should also be noted that the subroutine in the context of these investigations does not determine the α'-martensite content purely via the radial strain φ_r, but via the equivalent strain φ. Determining the radial strain φ_r would require another subroutine. However, since the radial strain has the largest share in the equivalent strain, the creation of another subroutine is omitted at this point. However, this represents a future work step.
To calculate the strain hardening, the approach according to [17] was used here without considering the temperature influence. In [17] the strain hardening due to martensite formation according to equation (3) is defined.

$$\sigma_{f,ges} = \sigma_y + \Delta\sigma_{y\rightarrow\alpha'} V_m \tag{3}$$

Here, the total resulting flow stress $\sigma_{f,ges}$ is given by the austenite flow stress σ_y and the strength increase due to the transformation into martensite $\Delta\sigma_{y\rightarrow\alpha'}$ in combination with the martensite fraction V_m.
For the strength increase of the austenite phase, the Hocket-Sherby approach is used [18]. Thus, overall, for the calculation of the yield stress considering the strain hardening, the equation (4) is obtained.

$$\sigma_{f,ges} = \left(B_{HS} - (B_{HS} - A_{HS})e^{-m\varphi^n}\right) + \Delta\sigma_{y\rightarrow\alpha'} V_m \tag{4}$$

Where A_{HS} is defined as the initial yield stress of the material and B_{HS} as the maximum yield stress, the latter being a theoretical value for infinitely large degrees of deformation. The parameters m and n are to be derived from experimentally determined austenite yield curves at different temperatures. For this investigation, the parameters in **Table 2** are used [19]. These were determined based on steel AISI 304 (1.4301), whose chemical composition lies within the tolerance range defined by the manufacturer for steel AISI 304L (1.4307) of the semi-finished product used here. The mechanical properties of the AISI

304L steel are identical despite the lowered carbon content. In the future, efforts will be made to determine these strength parameters for the semi-finished material. The implemented subroutine calculates the yield stress in each time increment for all integration points. Thus, the subroutine is also suitable for use with fully integrated elements, which would lead to an increase of computation time. The implemented subroutine is validated using a simplistic model, which is shown in Figure 6.

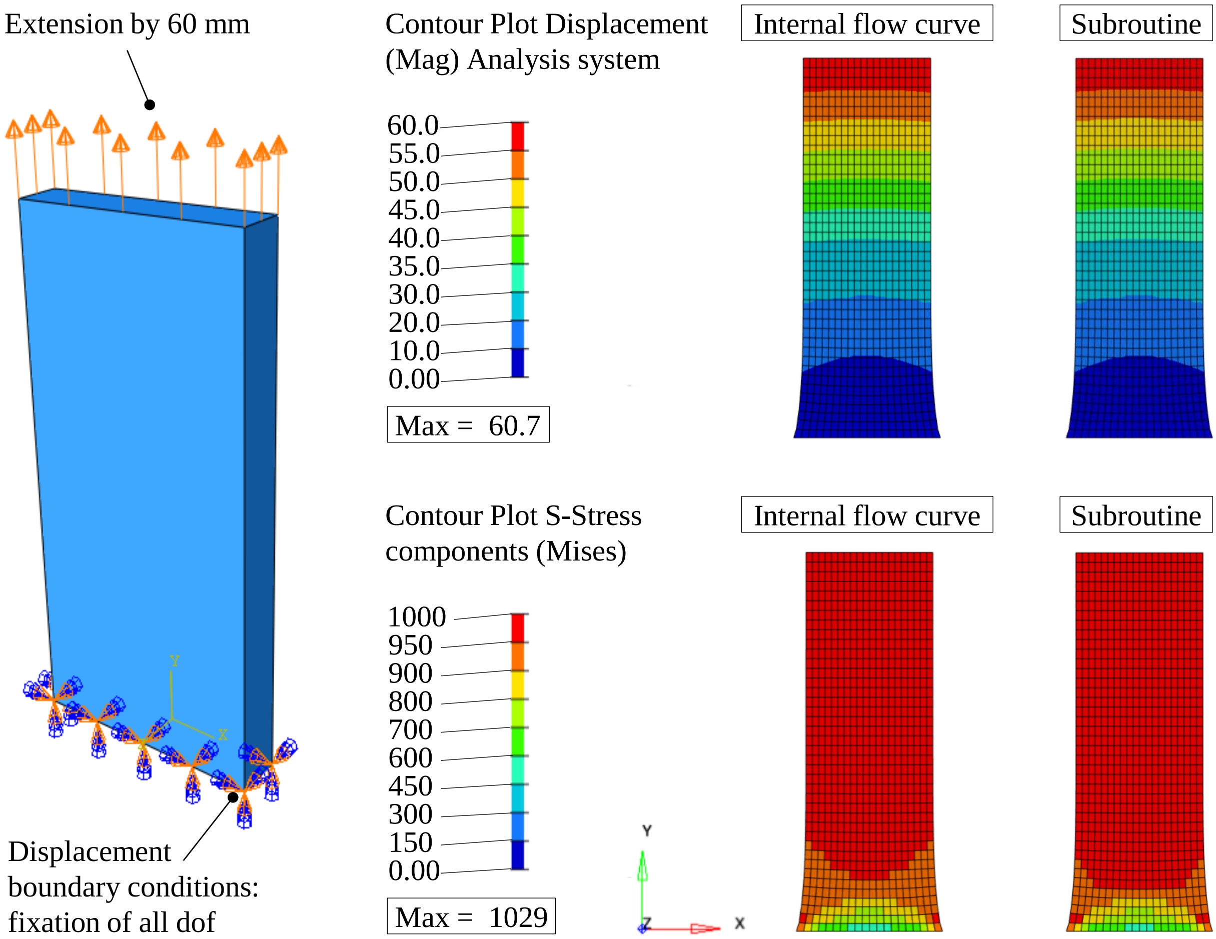

Figure 6. Contour Plot Displacement (Mag) Analysis system and Contour Plot S-Stress component (Mises) as substitute validation model.

For the validation, this substitute model is defined in order to reduce both its computation time and complexity, and thus to be able to properly assess the functioning of the subroutine. A rectangular cuboid is modeled with the material properties of the semi-finished product. At its bottom side, all degrees of freedom are locked with respect to the displacement boundary conditions. The upper side of the cuboid is extended by 60 mm. Subsequently, the load is relieved. This is used to evaluate the plastic behavior, which is controlled by the calculation of the yield stress. The yield curve, which is calculated by subroutine, is calculated manually for a parameter set for validation and stored in the Abaqus-internal material model. It should be noted that the manual calculation is accompanied by rounding errors, which must be considered when comparing the results with those of the subroutine. Figure 6 shows the comparison of the results of the simulation with and without the subroutine. The agreements of the stress as well as the plastic displacement show that the subroutine works correctly. As described before, rounding errors occur, which can be neglected. Furthermore, with the validation, an impression can be gained of the influence that the use of the subroutine has on the calculation time. With the substitute model listed here, the subroutine increased the calculation time by approximately 78%. Since the influence of the subroutine on the computation time increases as described before with increasing element number, it can already be assumed, by considering the substitute validation model from Figure **6**, that the computation time of the process model will increase significantly while using the subroutine.

Table 2. Parameters of the subroutine concerning equation (2) and (4).

Parameters for the calculation of martensite formation				
A_0	A_1	A_2	B_0	B_1
107.4	-107.67	0.2	1.05	-0.006
Parameters for the calculation of hardening				
A_{HS}	B_{HS}	m	n	$\Delta\sigma_{\gamma\to\alpha'}$
247.25	991.15	3.08	0.8979	572.86

4. Capabilities of process analysis with the FE model

In this study, initial analyses are carried out regarding the possibilities of process analysis with the FE model described in section 3.

Figure 7 shows the material flow of the semi-finished product during the forming process that can be represented by the modeling. A bulging and pile-up of material can be observed. Both phenomena are typical for reverse flow forming. For future investigations, it is necessary to validate these qualitatively correctly mapped phenomena quantitatively. However, the adequate representation of the material flow shows that process modeling offers the possibility to simulatively investigate the influence of different parameters, such as the feed rate, the rotational speed and the roller tools infeed, on the bulging and pile-up of material.

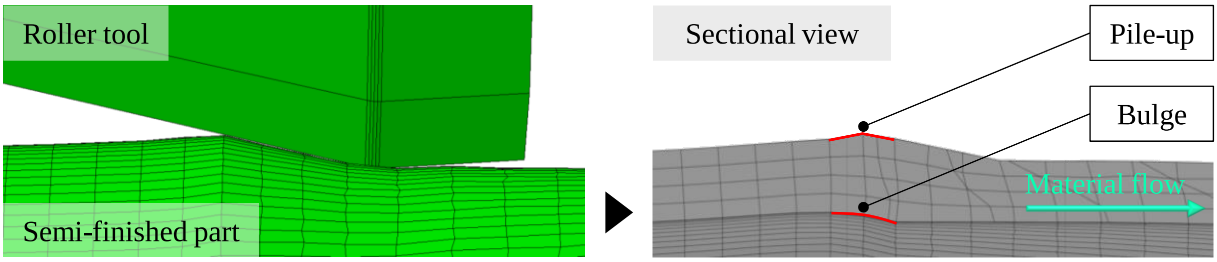

Figure 7. Simulative material flow: Bulging and pile-up of material.

Furthermore, in addition to the determination of common quantities such as strains as well as stresses, the 3D process modeling enables the determination of the α’-martensite content of the entire component over the entire process time. The work hardening resulting from the α’-martensite formation is also considered. In addition, the determination is also possible via the wall thickness of the semi-finished product, as shown in Figure 8.

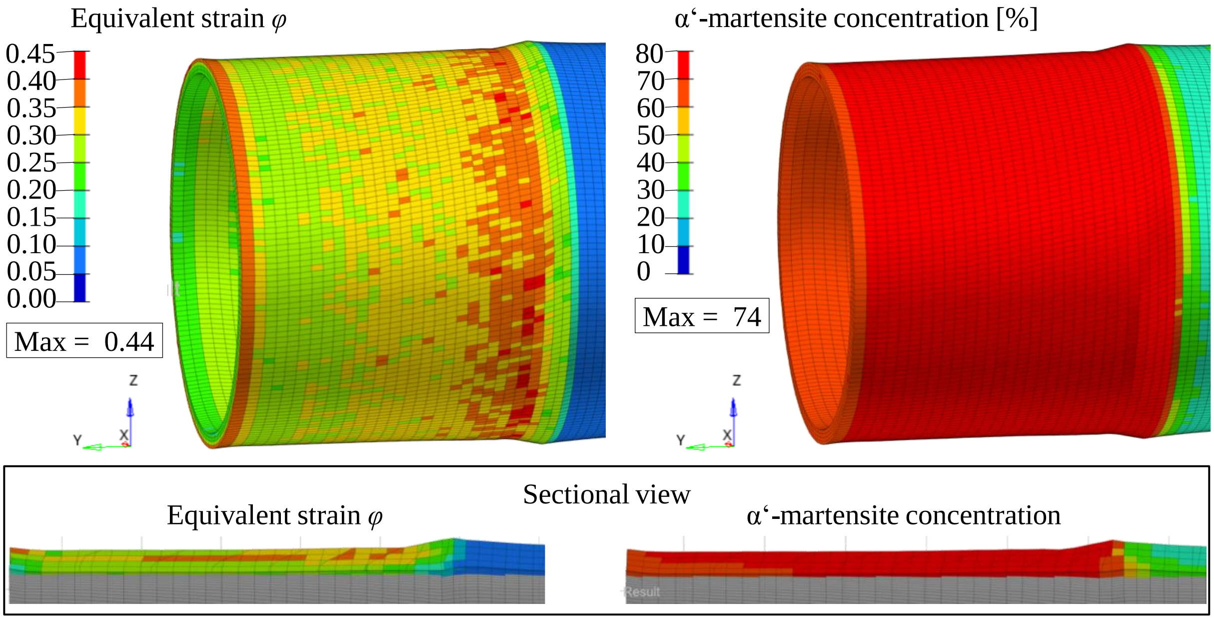

Figure 8. Contour plots of equivalent strain and α’-martensite concentration determined by the FE process model for reverse flow forming.

The application of the process model with implemented subroutine show that very high calculation times occur. Here the calculation time is influenced by certain factors. One factor is the space discretization. Thus, an increasing number of elements as well as a decreasing characteristic element size negatively influences the maximum permissible time step. CEL meshing also increases the computation time. Another factor is the use of the subroutine, the influence of which has already been described in detail. In addition, the reverse flow forming process has comparatively long process times. For a specimen with a length of 100 mm, which is formed with a feed rate of 60 mm/min, a process time of over 100 s results with the infeed of the roller tools. In contrast, the maximum permissible time step for the process setup described in section 3 is about $8.9 \cdot 10^{-8}$ s. It should be noted here that the process modeling will be extended for other combinations of feed rate and speed. In this case, lower feed rates and higher speeds than those assumed here will have an additional negative effect on the calculation time.
Therefore, the reduction of the calculation times, e.g., in the form of scaling possibilities, plays an important role for future investigations. In this context, it is important to investigate which possibilities exist for computation time reduction and how the respective measure affects the solution quality. Two possible approaches are time scaling and mass scaling. Here it can already be said that the mass scaling of the CEL approach is only possible if the critical time step is determined by the Lagrangian mesh. More likely, the maximum permissible time step is defined by the Eulerian mesh, which does not enable mass scaling. Therefore, the scaling possibilities in connection with alternative space discretization approaches must be investigated additionally.

5. Model-based closed-loop process control

The FEM is a suitable, powerful modelling method for flow forming process modelling and martensite formation that could be used to predict forming results depending on process parameters like a defined toolpath and -velocity, as sawn from the results in the sections above. Nevertheless, even an accurate process model distinguishes from the actual forming process by model simplifications for acceptable computation costs and time, model uncertainties, and process disturbances. This is for example due to unmodelled elastic resilience of the forming machine, slight variations of the ambient temperature during the process, initial imperfections within the semi-finished tubes like an eccentricity or inhomogeneous microstructure. Iterative, model-based toolpath planning for the actual process thus leads to deviations between the desired and the resulting workpiece. The authors already proposed an online closed-loop property and process control to counter this challenge (see [9, 20]). Closed-loop control in this context means to control the resulting workpiece properties themselves, additionally to the actuators. The general closed-loop control concept for flow forming of metastable austinites is subsequently presented in Figure 9.

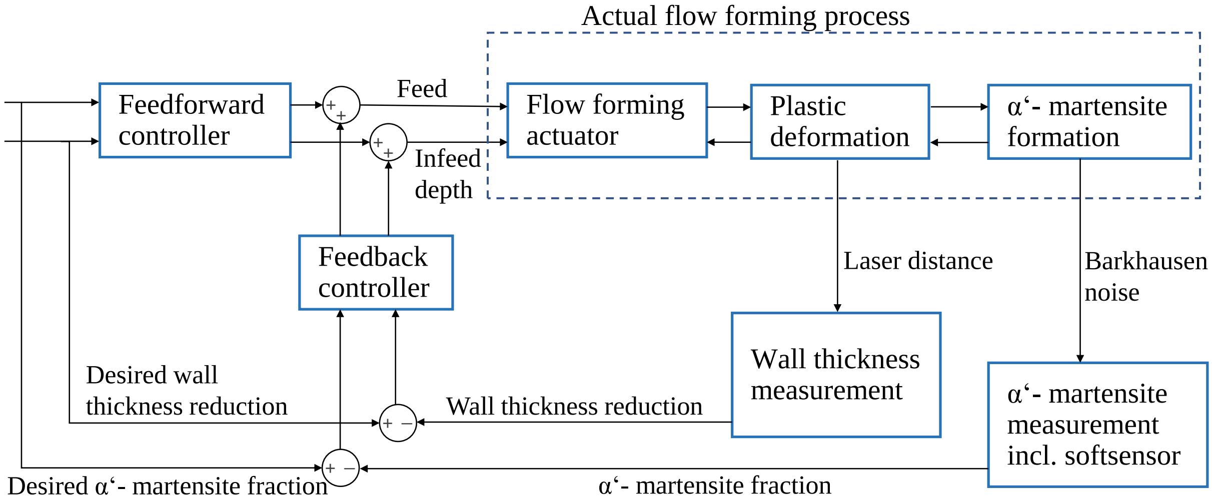

Figure 9. Closed-loop online control concept for flow forming of metastable austenites.

During the forming on the actual machine, the workpiece is monitored by moving sensors coupled with the machine support and measuring the actual workpiece properties: two laser distance sensors for the wall thickness reduction to ensure the workpiece geometry and a micromagnetic (soft-)sensor to supervise the α'-martensite fraction (see also [9, 20]). The wall thickness reduction Δw here is calculated by the difference between the wall thickness in the unformed workpiece area w_0 and the formed section w_1. The micromagnetic Barkhausen noise is measured and correlated to the α'-martensite fraction via a softsensor (see [9]). The actuator toolpath – radial infeed depth Δr and axial feed f of the roller tool – is planned offline before forming in a feed forward controller and continuously adjusted online during the forming by the controller depending on the measured sensor signals.
The proposed closed-loop control concept has already been applied to an actual forming machine. It was successfully validated for the measured wall thickness reduction Δw as the control variable, the infeed depth Δr as the manipulated variable and a constant feed f in previous investigations of the authors. For designing the controller, a novel system model presented in [20] was used in MATLAB/Simulink as a proof of concept. This system model of the flow forming process includes a discretization of the workpiece, an empirical black-box plastic deformation model, the Olson-Cohen-based material model of martensite formation (see section 2.3), a sensor model and the control loop, but force-related effects like friction and residual stresses were disregarded. For this reason, the actual system model is less accurate than the FE model that includes these effects. It is thus planned to enhance the system model accuracy by integrating the novel flow forming FE process model. However, this model coupling of the system simulation and FEM depicts a challenge because of the different simulation duration: System simulation amounts a duration of less than 1 minute using the system model from [20]. The presented FE model requires days of simulation time for calculation by contrast. Hence, the resulting computation costs of the FEM would be far too great for efficient control design. A possible solution to overcome this challenge, which has to be investigated in the future, could be to directly export a reduced order model from the FEM into the MATLAB/Simulink system model, as Roncarati and Oetinger in [21] and [22] already have successfully demonstrated. It is tentatively planned to adapt this approach to a model order reduction of the (single pass) reverse flow forming process model from this paper. The preliminary model concept for the resulting flow forming system model including the reduced order process model is presented in Figure 10.

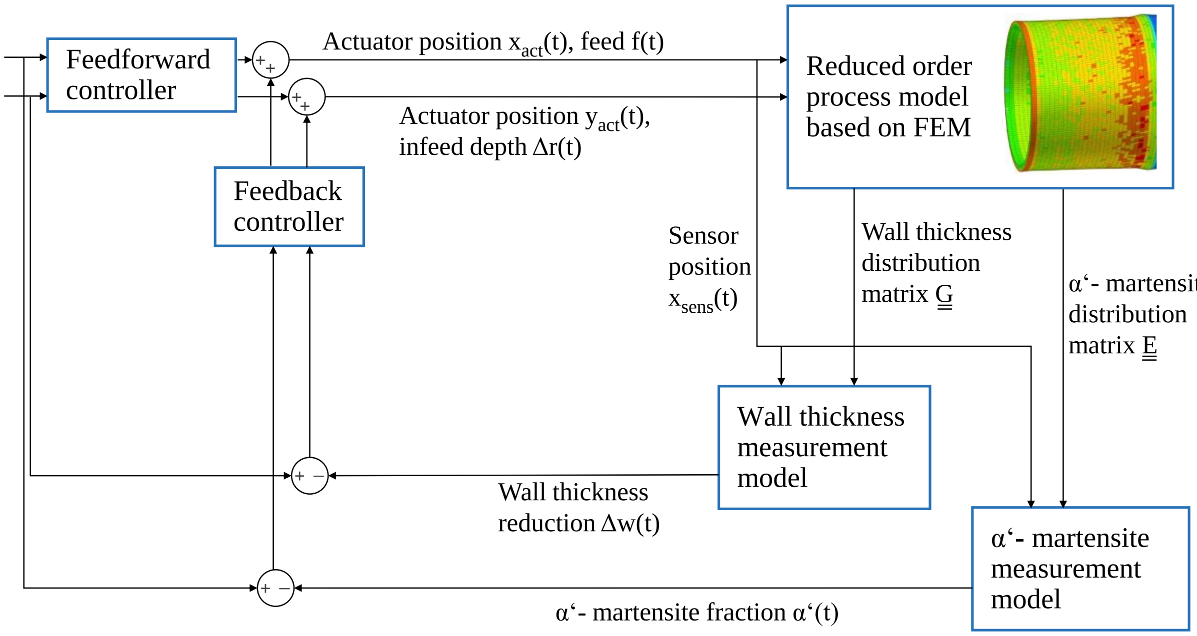

Figure 10. Advanced system model concept including integrated reduced order model based on FEM.

Here, the black-box plastic deformation model from the initial system model would be replaced by the new reduced order process model. In this way, the system model could be evolved into a grey-box model. In the potential concept, the material model is also formally removed from the system model and is now a part of the FE process model within a subroutine, while sensor model and control remain. However, the feasibility and accuracy of this refined modeling approach (especially considering the incremental process character of flow forming) will be part of further research.
Using the described modeling approach is expected to increase the accuracy of the system model and still reduce time and costs in the model-based control design process. The tool trajectory in the feedforward controller could then be determined offline with the model by defining an optimization problem minimizing the deviation between simulation result and setpoint of a defined wall thickness or α'-martensite distribution over different simulated toolpaths, for example. The calculated tool trajectory can then be programmed into the actual forming machine and used for manufacturing. Thus, the online (feedback) controller in the machine only has to control deviations from the model caused by simplifications, uncertainties and process disturbances. Additionally, the model-based feedforward controller could be adapted online during the forming process. After each incremental pass, the planned tool path would be updated by repeating the optimization process considering the measured, actual workpiece properties. Thus, it will become possible to compensate those remaining errors from the previous pass, which the online feedback controller did not correct.

6. Conclusions and outlook

Within the scope of these investigations, the creation of an FE process modeling for reverse flow forming using ABAQUS/EXPLICIT was presented, which, through the implementation of a subroutine, considers the α'-martensite formation and associated work hardening that occurs during forming. In addition to the description of this modeling, its range of validity and the subroutine, the resulting boundary conditions that the process imposes on the FE modeling were highlighted. Subsequently, the possibilities of the process analysis with the help of this model were pointed out and optimization approaches and future objects of investigation were discussed.
The goal is to extend the FE modeling to the entire process with multiple passes and flexible parameter settings. For this purpose, additional investigations are necessary beforehand. Thus, further approaches of space discretization in connection with adequate scaling possibilities to reduce the computation time have to be investigated as well as compared. In addition, a supplementary subroutine should be

implemented so that only the radial degree of deformation is considered in the calculation of the α'-martensite formation. Regarding the work hardening, it is recommended to determine the strength parameters explicitly for the semi-finished material. In addition, it is conceivable to investigate and, if necessary, implement further approaches for the analytical description of strain hardening. It is extremely important to validate the process model by means of experimental process investigations so that the validation can be carried out qualitatively and quantitatively.
In addition, an approach for implementing the FE process model within the proposed closed-loop process control in a predictive sense was demonstrated. It is necessary to verify how useful the use of the FEM is in this context and whether the hoped-for added value will be given. With regard to the calculation time, it is necessary to check to what extent an approximation to the calculation time of the MATLAB/Simulink system model is possible. Furthermore, it is important to examine how the direct comparison of the MATLAB/Simulink system model with the FE model performs in terms of model quality, since the idealizations have led to a certain model fuzziness.

References

[1] Yang D, Bambach M, Cao J, Duflou J, Groche P, Kuboki T, Sterzing A, Tekkaya A and Lee C 2018 Flexibility in metal forming *CIRP Annals* **67**, Issue 2, pp. 743-765, DOI: 10.1016/j.cirp.2018.05.004
[2] Ingarao G, Di Lorenzo R and Micari F 2011 Sustainability issues in sheet metal forming processes: An overview *Journal of Cleaner Production* **19**, Issue 4, pp. 337-347, DOI: 10.1016/j.jclepro.2010.10.005
[3] Mohebbi M S and Akbarzadeh A 2010 Experimental study and FEM analysis of redundant strains in flow forming of tubes *Journal of Materials Processing Technology* **210**, Issue 2, pp. 389-395, DOI: 10.1016/j.jmatprotec.2009.09.028
[4] Knigge J 2015 Lokale Martensitbildung in metastabilen austenitischen Stählen durch Verfahren der Massivumformung Dissertation *Berichte aus dem IFUM* **2**/2015
[5] Talonen J 2007 Effect of strain-induced α'-martensite transformation on mechanical properties of metastable austenitic stainless steel *Doctoral Dissertation*, Helsinki University of Technology
[6] Arian B, Homberg W, Riepold M, Trächtler A, Rozo V J and Walther F 2021 Forming of metastable austenitic stainless steel tubes with axially graded martensite content by flow forming, *ESAFORM 2021, 24th Int. Conf. on Material Forming (Liège)*, DOI: 10.25518/esaform21.2759
[7] Runge M 1994 *Spinning and Flow forming: spinning and flow forming technology, product design, equipment, control systems* (Landsberg/Lech: Verlag Moderne Industrie)
[8] Sivanandini M, Dhami S S and Pabla B S 2012 Flow forming of tubes: A review *Int. Journal of Scientific and Engineering Research* **3**, Issue 5, pp. 587-597
[9] Riepold M, Arian B, Rozo V J, Homberg W, Walther F and Trächtler A 2021 Model approaches for closed-loop property control for flow forming *Advances in Industrial and Manufacturin Science* **3**, DOI: 10.1016/j.aime.2021.100057
[10] Marini D, Cunningham D, Xirouchakis P and Corney J 2016 Flow forming: A review of research methodologies, prediction models and their applications *Int. Journal of Mechanica Engineering and Technology* **7**, Issue 5, pp. 285-315, DOI: 10.25518/esaform21.2759
[11] Bylya O I, Khismatullin T, Blackwell P and Vasin R A 2018 The effect of elasto-plastic properties of materials on their formability by flow forming *Journal of Materials Processing Technolog* **252**, pp. 34-44, DOI: 10.1016/j.jmatprotec.2017.09.007
[12] Weidner A 2020 Deformation processes in TRIP/TWIP steels (Springer International Publishing)
[13] Olson G B and Cohen M 1975 Kinetics of strain-induced martensitic nucleation *Metallurgicaland Materials Transactions A* **6**, pp. 791-795, DOI: 10.1007/BF02672301
[14] Mansourinejad M and Ketabchi M 2017. Modification of Olson-Cohen model for predicting stress-state dependency of martensitic transformation *Materials Science and Technology* **33**, Issue 16, pp. 1948-1954, DOI: 10.1080/02670836.2017.1342016
[15] Smaga M, Walther F and Eifler D 2006 Investigation and modelling of the plasticity-induced martensite formation in metastable austenites *Int. Journal of Materials Research* **97**, 12, pp. 1648-1655, DOI: 10.3139/146.101396

[16] Dassault Systems 2014 Abaqus user subroutines reference guide
[17] Hänsel A 1998 *Nichtisothermes Werkstoffmodell für die FE-Simulation von Belchumformprozessen mit metastabilen austenitischen CrNi-Stählen* Doctoral Dissertation, ETH Zürich
[18] Hockett J E and Sherby O D 1975 Large strain deformation of polycrystalline metals at low homologous temperatures *Journal of the Mechanics and Physics of Solids* **23**, Issue 2, pp. 87-98, DOI: 10.1016/0022-5096(75)90018-6
[19] Krauer J 2010 *Erweiterte Werkstoffmodelle zur Beschreibung des thermischen Umformverhaltens metastabiler Stähle* Doctoral Dissertation, ETH Zürich, DOI: 10.3929/ethz-a-006234345
[20] Kersting L, Arian B, Rozo V J, Trächtler A, Homberg W and Walther F 2022 *Innovative online measurement and modelling approach for property-controlled flow forming processes (accepted), ESAFORM 2022, 25th Int. Conf. on Material Forming (Braga)*
[21] Roncarati L 2014 *Model order reduction and system simulation of a machine tool for real-time compensation of thermally induced deformations, ANSYS Conference & 32. CADFEM Users' Meeting 2014 (Nürnberg)*
[22] Oetinger D, Sawodny O 2015 *Using model order reduction for disturbance feed forward control based on transient thermal finite element models 2015 IEEE Conference of Control Applications (CCA*), pp. 1486-1491, DOI: 10.1109/CCA.2015.7320821

Acknowledgments
The authors would like to thank the German Research Foundation (Deutsche Forschungsgemeinschaft, DFG) for their support of the depicted research within the priority programme SPP 2183 “Property-controlled metal forming processes”, through project no. 424335026 “Property control during spinning of metastable austenites”.